

Accelerated Articles

Reduction of Signal Suppression Effects in ESI-MS Using a Nanosplitting Device

Eric T. Gangl,^{†,‡} Meg Annan,[§] Neil Spooner,[§] and Paul Vouros^{*,†}

Barnett Institute and Department of Chemistry, Northeastern University, Boston, Massachusetts 02115, and GlaxoSmithKline Pharmaceuticals, King of Prussia, Pennsylvania 19406

Electrospray ionization mass spectrometry is a valuable tool in the identification and quantification of drug metabolites in biological fluids. However, there are many instances where matrix components present in these fluids interfere with analyte detection and prevent the acquisition of accurate or complete results. In some instances, the matrix can suppress ionization to such an extent that analytes are completely undetectable by MS. In this work, we investigate how ionization and ion-transfer efficiencies are affected by drastically reducing the flow into the MS. A postcolumn concentric flow-splitting device was constructed to allow the measurement of analyte signal and ionization suppression across a range of flow rates (0.1–200 $\mu\text{L}/\text{min}$). Using this device, the effects of flow rate on signal intensity and ionization suppression were measured in analytical experiments that included flow injection analysis MS, postcolumn addition LC–MS, and on-line LC–MS analysis of metabolites generated from rat liver microsomes. The device used to deliver 0.1 $\mu\text{L}/\text{min}$ flows is referred to as a nanosplitter because it achieved high split ratios (2000:1), producing flow rates comparable to those observed in nanoelectrospray. The nanosplitter maintained chromatographic integrity with high fidelity and allowed the direct comparison of analyte signal across a range of flow rates (0.1–200 $\mu\text{L}/\text{min}$). A significant improvement in concentration and mass sensitivity as well as a reduction in signal suppression is observed when the performance at 200 versus 0.1 $\mu\text{L}/\text{min}$ flow rate is compared. Using this specially designed concentric splitting device, the advantages of

ultralow flow ESI were easily exploited for applications employing large bore chromatography.

High-performance liquid chromatography–mass spectrometry (LC–MS) is a widely applied technique for the fast and sensitive characterization and quantification of pharmaceutical compounds and their metabolites.¹ The analysis of these agents in complex biological fluids such as plasma, urine, bile, feces, and tissue homogenates for the determination of pharmacokinetic parameters and metabolic pathways is a crucial step in the drug development process.^{2–6} The inherent specificity of mass detection coupled with the component separation afforded by chromatography has contributed to increased analytical productivity in the area of quantitative analysis by reducing the need for extensive sample preparation. In addition, the unique combination of detection sensitivity and information content has made LC–MS an essential tool in the determination of metabolic pathways. These tools have resulted in reduced assay development times, analysis times, and detection limits. In fact, the literature has shown that several thousand quantitative assays can be carried out in a single day through the use of 96-well plate technology and tandem mass spectrometric (MS/MS) techniques.^{2,7–10} Furthermore, developments in software applications have enabled the automated

- (1) Wilm, M.; Mann, M. *Anal. Chem.* **1996**, *68*, 1–8.
- (2) Adams, D. A.; Murray, S.; Clifford, C. P.; Rendell, N. B.; Davies, D. S.; Taylor, G. W. *J. Chromatogr., B: Biomed. Sci. Appl.* **1997**, *693*, 345–51.
- (3) Bootsma, A. H.; Overmars, H.; van Rooij, A.; van Lint, A. E.; Wanders, R. J.; van Gennip, A. H.; Vreken, P. *J. Inherited Metab. Dis.* **1999**, *22*, 307–10.
- (4) Carrascal, M.; Schneider, K.; Calaf, R. E.; van Leeuwen, S.; Canosa, D.; Gelpi, E.; Abian, J. *J. Pharm. Biomed. Anal.* **1998**, *17*, 1129–38.
- (5) Heinig, K.; Henion, J. *J. Chromatogr., B: Biomed. Sci. Appl.* **1999**, *735*, 171–88.
- (6) Majumdar, T. K.; Bakhtiar, R.; Melamed, D.; Tse, F. L. *Rapid Commun. Mass Spectrom.* **2000**, *14*, 476–81.
- (7) Jemal, M.; Teitz, D.; Ouyang, Z.; Khan, S. *J. Chromatogr., B: Biomed. Sci. Appl.* **1999**, *732*, 501–8.
- (8) Davies, I. D.; Allanson, J. P.; Causon, R. C. *J. Chromatogr., B: Biomed. Sci. Appl.* **1999**, *732*, 173–84.

* Corresponding author: (phone) 617-373-2794; (fax) 617-373-2693.

[†] Northeastern University.

[‡] Current address: Vertex Pharmaceuticals, Cambridge, MA 02139.

[§] GlaxoSmithKline Pharmaceuticals.

quantitative and qualitative characterization of drugs and metabolites, thus alleviating the bottleneck in data processing generated by increased sample throughput. The use of LC-MS-based methodologies has therefore become popular and widespread in the pharmaceutical industry as evidenced by the breadth and volume of publications within this sector.^{2,7,8} While these analytical techniques have enjoyed tremendous success in recent years, there have been many instances where they have faltered.¹¹⁻¹³

Efforts to increase sample throughput have placed huge demands on analytical instrumentation to obtain error-free measurements over long periods of time. In many instances, matrix components present in these samples are responsible for analysis failures and errors. Not only do these components foul instrumentation but they also interfere with detection processes in mass spectrometry. Because ion transmission is generally dependent upon mass and mass-to-charge ratio and not analyte structural features, problems with analyte detection have often been attributed to processes in the electrospray ionization (ESI) region of the mass spectrometer, such as ionization suppression by matrix components.^{14,15} The mechanism by which matrix components suppress analyte signal is not fully understood; however, several noteworthy hypotheses have been reported.^{11,16,17} In particular, many components in biological fluids such as ionic salts and bile acids of either very large relative abundance, very high ionization efficiency, or high surface activity can reduce the analyte response such that the quality of analytical measurements is compromised. In extreme cases, components in matrixes such as bile can cause ionization suppression to such an extent that the major metabolites are rendered undetectable by MS. Time-consuming sample preparation methods have often been inadequate because they only remove a portion of the matrix components.¹¹ For example, solid-phase extraction (SPE) methods are only moderately successful at limiting suppression effects because they rely on large differences in chromatographic behavior for matrix removal. Matrix components that remain following SPE cleanup typically have chromatographic behavior similar to that of the analyte(s). As a result, these components are likely to coelute with the analyte in LC-MS and continue to cause ionization suppression.

It has been shown that reducing the ESI flow rate to the nanoliter per minute range leads to increased desolvation, ionization, and ion-transfer efficiency over ESI conducted at higher flow rates.¹ The high degree of sensitivity demonstrated by this technique has provoked much research into the design, construction, and evaluation of these nanoelectrospray sources.¹⁸⁻²¹ As an example, Bahr et al. demonstrated that carbohydrates, which

typically require chemical derivatization for suitable sensitivity in ESI-MS,²² can be detected as readily as peptides when analyzed under nanospray conditions.¹⁶ It has been hypothesized that the smaller droplet size achieved by nanospray forces the hydrophilic carbohydrate molecules closer to the droplet surface, thus causing them to behave like the more surface-active peptides. Furthermore, the higher surface-to-volume ratios of the smaller nano-ESI droplets result not only in improved concentration sensitivity but also in resistance to ionization suppression effects. In agreement with this theory, Juraschek et al. reported that nanoelectrospray is more tolerant of samples that contain a nonvolatile salt (e.g., NaCl) because of its ability to generate smaller, more highly charged droplets.²³

In the context of nanoelectrospray and its benefits, we have utilized a modification of the experimental methodology of Bonfiglio et al.,¹¹ whereby the effect of eluting matrix components on the response of a postcolumn infusion of analyte could be measured. In the process of adapting this methodology to our investigations, we have designed a novel flow-splitting device that is capable of achieving extremely high split ratios (>2000:1) without peak broadening. Hence, we refer to this device as a nanosplitter because it can achieve flow rates in the nanoliter per minute range by splitting from bulk flows as high as 1 mL/min and thereby allowing the analysis of samples (e.g., neat bile) which may cause problems when analyzed with capillary LC columns. In this work, ionization suppression effects were evaluated across a wide range of flow rates and using an array of different suppressing agents. The primary goal of this work was to determine whether lower ESI flow rates, especially in the nanoliter per minute range, would lead to reduced ionization suppression and improved concentration sensitivity. Analyte signal suppression was examined both qualitatively and quantitatively through the use of the aforementioned splitting device developed in our laboratory. Demonstration of signal suppression and resistance to signal suppression was accomplished using three types of experiments each conducted at several flow rates.

The experiments were based on flow injection analysis (FIA) MS, postcolumn addition (PCA) LC-MS, and on-line LC-MS analysis of metabolites from *in vitro* sources. While the exact details for these experiments are presented in the Experimental Section, a brief description is given here. The first experiment was based on the flow injection of a test analyte either alone (benchmark signal) or in the presence of an excess amount of a suspected suppressing agent. The test analyte was Carvedilol and the suppressing agents were dimethyl sulfoxide (DMSO), Indinavir, and taurocholic acid (TCA; Figure 1). Conclusions on suppression effects were drawn by comparing the signal from the benchmark solution with the signals obtained from the solutions containing test analyte and a suppressing agent. In the second experiment, the LC column effluent following injection of a blank

- (9) Onorato, J. M.; Henion, J. D.; Lefebvre, P. M.; Kiplinger, J. P. *Anal. Chem.* **2001**, *73*, 119-25.
- (10) Zweigenbaum, J.; Henion, J. *Anal. Chem.* **2000**, *72*, 2446-54.
- (11) Bonfiglio, R.; King, R. C.; Olah, T. V.; Merkle, K. *Rapid Commun. Mass Spectrom.* **1999**, *13*, 1175-85.
- (12) Constantopoulos, T. L.; Jackson, G. S.; Enke, C. G. *J. Am. Soc. Mass Spectrom.* **1999**, *10*, 625-34.
- (13) Eshraghi, J.; Chowdhury, S. K. *Anal. Chem.* **1993**, *65*, 3528-33.
- (14) Enke, C. G. *Anal. Chem.* **1997**, *69*, 4885-93.
- (15) Sterner, J. L.; Johnston, M. V.; Nicol, G. R.; Ridge, D. P. *J. Mass Spectrom.* **2000**, *35*, 385-91.
- (16) Bahr, U.; Pfenninger, A.; Karas, M.; Stahl, B. *Anal. Chem.* **1997**, *69*, 4530-5.
- (17) King, K.; Bonfiglio, R.; Fernandez-Metzler, C.; Miller-Stein, C.; Olah, T. J. *Am. Soc. Mass Spectrom.* **2000**, *11*, 942-50.
- (18) Davis, M. T.; Stahl, D. C.; Hefta, S. A.; Lee, T. D. *Anal. Chem.* **1995**, *67*, 4549-56.

- (19) Hsieh, F.; Baronas, E.; Muir, C.; Martin, S. A. *Rapid Commun. Mass Spectrom.* **1999**, *13*, 67-72.
- (20) Wachs, T.; Sheppard, R. L.; Henion, J. *J. Chromatogr., B: Biomed. Appl.* **1996**, *685*, 335-42.
- (21) Wahl, J. H.; Gale, D. C.; Smith, R. D. *J. Chromatogr., A* **1994**, *659*, 217-22.
- (22) Burlingame, A. L.; Boyd, R. K.; Gaskell, S. J. *Anal. Chem.* **1998**, *70*, 647R-716R.
- (23) Juraschek, R.; Dulcks, T.; Karas, M. *J. Am. Soc. Mass Spectrom.* **1999**, *10*, 300-8.

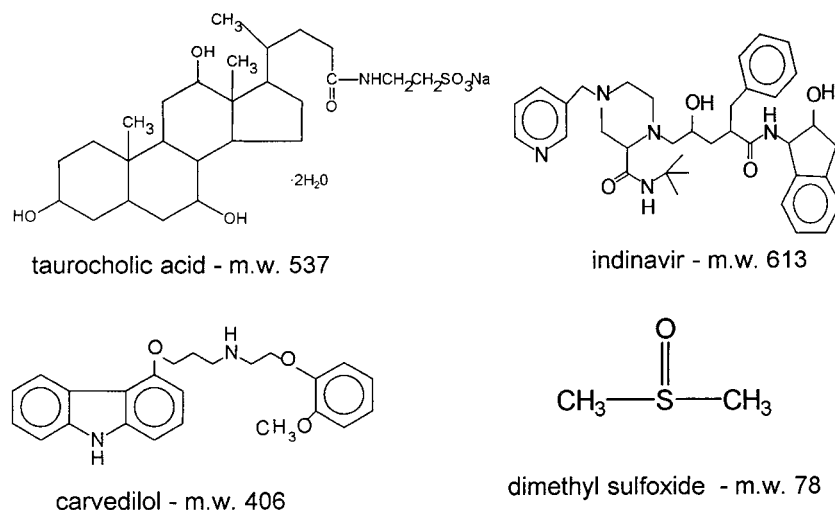


Figure 1. Structures of (A) taurocholic acid as the sodium salt, (B) Indinavir, (C) Carvedilol, and (D) dimethyl sulfoxide.

matrix solution (bile) was “teed” into a postcolumn addition of the test analyte, Carvedilol. The Carvedilol baseline signal was then modulated according to the nature of the column effluent. The effect of the eluting matrix components was evaluated at different ESI flow rates using the nanosplitter. It should be emphasized here that the chromatographic flow was always constant at 0.200 mL/min. A change in “flow rate” therefore refers only to the flow of sample into the ionization source of the mass spectrometer, also called “ESI flow”. The last experiment conducted mimicked the real world application of analyzing metabolites derived from in vitro incubations. Injections of Indinavir metabolites were made onto an LC–MS system. The effect of different ESI flow rates on the analysis of a real sample was evaluated using the novel concentric nanosplitter to adjust the delivery of flow to the MS.

EXPERIMENTAL SECTION

Chemicals. All water used was purified with a Milli-Q water filtration system, Millipore, (Bedford, MA). Carvedilol, as the free base (>99% purity), was obtained from GlaxoSmithKline pharmaceuticals (King of Prussia, PA). Indinavir, as the sulfate salt (>98% purity by HPLC), was a gift from Merck Research Laboratories (West Point, PA). Ammonium acetate, acetic acid, dimethyl sulfoxide, and taurocholic acid (as the sodium salt) were obtained from Sigma (St. Louis, MO). All solvents were HPLC grade unless otherwise specified. Methanol was obtained from EM Science (Gibbstown, NJ), and acetonitrile was obtained from J. T. Baker (Phillipsburg, PA).

Metabolite Preparation. Rat liver microsomes were prepared as previously described,²⁴ and protein was determined by the method of Lowry et al.²⁵ All microsomal incubations were conducted in a shaking water bath at 37 °C. They contained liver microsomal protein (2.1 mg/mL), NADPH (1 mM), and Indinavir (10 μM) in 50 mM potassium phosphate buffer, pH 7.4. Incubations with no NADPH served as the controls. Total volume of the incubation was 10 mL. The incubation of Indinavir with rat liver microsomes was terminated after 4 h. The metabolites were

extracted by shaking the incubation mixtures with 20 mL of methylene chloride. The incubations were stopped by addition of an equivalent volume of 80:20 MeOH/2-propanol containing 1% acetic acid. The resulting solution was not extracted or dried, but simply vortexed and spun down at ~12g. The supernatant was decanted and diluted with water as described below.

HPLC. A HP series 1090 HPLC with an autosampler and diode array detector (Agilent Technologies, Palo Alto, CA) was used for FIA and HPLC experiments. The HPLC system was controlled with HP ChemStation software (version A.06.03) running on an IBM-compatible PC. For all HPLC experiments, a Waters (Milford, MA) Symmetry C₁₈ reversed-phase LC column (2.1 mm × 10 cm × 3.5 μm) was used and the effluent was monitored by UV at 210, 230, and 254 nm with DAD spectra acquired every 0.5 s. To prevent salt contamination of the ESI source during bile injections, the column effluent was diverted to waste for the first 2.2 min of the run.

Mass Spectrometry. Mass spectrometric measurements were conducted with a TSQ 700 triple quadrupole mass spectrometer (Finnigan MAT, San Jose, CA) controlled with UNIX operating system (version 4 F), running ICIS 8.3, and ICL version 7.5. The mass spectrometer was calibrated using the manufacturer recommended MRFA–myoglobin solution. To maximize the sensitivity for the detection of Carvedilol and Indinavir, tuning was performed at each of the flow rates (50, 5, and 0.1 μL/min). This ensured that the mass spectrometer was optimally tuned for the analyte at each flow rate. In these tuning procedures, Carvedilol (*m/z* 407) or Indinavir (*m/z* 614) was infused at 0.1, 5, and 50 μL/min at concentrations of 1 μg/mL in 80% CH₃OH, 20% H₂O, and 0.1% CH₃COOH (v/v/v). A syringe pump (model 980532, Harvard Apparatus, Holliston, MA) with appropriate volume syringe was used in the infusion experiments.

ESI and Concentric Splitting Device. The standard Finnigan electrospray interface was used (+3.8 to +4.2 kV) where the heated capillary was held at 200, 225, and 225 °C for the 5, 50, and 200 μL/min flow rates, respectively. The standard Finnigan 150-μm-i.d. stainless steel ESI sprayer was used for these flow rates. Dry nitrogen gas (25 psi of sheath gas and 5 psi of auxiliary gas) was used as the nebulization/drying gas.

(24) Koudriakova, T.; Iatsimirskaya, E.; Utkin, I.; Gangl, E.; Vouros, P.; Storozhuk, E.; Orza, D.; Marinina, J.; Gerber, N. *Drug Metab. Dispos.* **1998**, *26*, 552–61.

(25) Lowry, O. H.; Rosebrough, N. J.; Farr, A. L.; Randall, R. J. *J. Biol. Chem.* **1951**, *193*, 265–75.

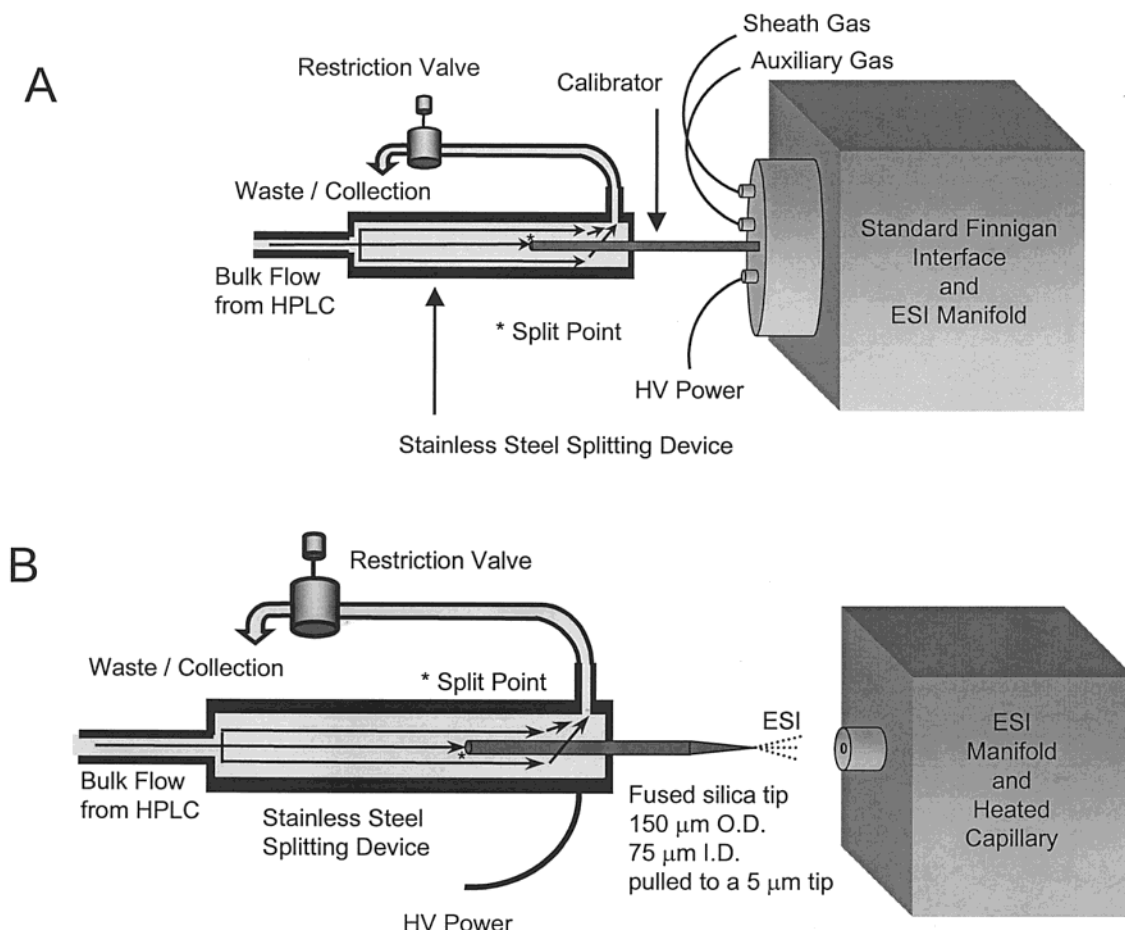


Figure 2. (A) Concentric splitting device used with the standard Finnigan ESI interface at 50 and 5 $\mu\text{L}/\text{min}$ flow rates. (B) Nanosplitting device used for split ratios of $\geq 1000:1$ (nanosplitter).

For splitting at 5 and 50 $\mu\text{L}/\text{min}$, a custom-built concentric splitting device composed of several individual parts was used (Figure 2A). The splitter was used in conjunction with a length of constant-bore fused-silica tubing (Polymicro Technologies, Phoenix AZ) for the split flow exiting toward the ESI-MS system. This piece of tubing, typically referred to as a calibrator, coarsely determined the split ratio from a predetermined input flow. The 5 $\mu\text{L}/\text{min}$ calibrator had dimensions (i.d. \times length) of 50 $\mu\text{m} \times 28.6$ cm, while the 50 $\mu\text{L}/\text{min}$ calibrator had dimensions of 75 $\mu\text{m} \times 22.9$ cm. A needle valve (86041, Alltech, Deerfield, IL), placed on the waste side of the splitter, enabled fine adjustment of split ratios by regulating back pressure within the splitter. For these flow-splitting experiments, the bulk flow from the HPLC was introduced to the splitter and the majority was sent to waste through the vent/waste port. The remainder of the flow was directed through the split orifice toward the MS. The flow exiting the splitter (MS flow side) was collected in a syringe with volumetric markings and was used to determine the flow rate (μL) per unit time (min) toward the MS.

For the 0.1 $\mu\text{L}/\text{min}$ flow rate, the Finnigan source was replaced with an integrated splitter-ESI system designed and constructed in-house (Figure 2b). The device was designed to enable easy and reliable splitting of bulk flow rates (200–1000 $\mu\text{L}/\text{min}$) down to nanospray conditions (≤ 0.1 $\mu\text{L}/\text{min}$), hence it is referred to as a "nanosplitter". It consisted of an XYZ positioner (FP-2 Newport, Irvine, CA), a splitter (FSMUAS1.5, Valco Instruments Co. Inc.,

Houston, TX), and a needle valve (86041, Alltech) all fastened to a rail and mount system (9742(M) New Focus, Inc., Sunnyvale, CA) and fitted to the TSQ 700. Once again, the needle valve functioned to finely adjust split ratios by regulating back pressure within the splitter. The high-voltage connection was made using an alligator clip attached to the stainless steel body of the splitter. For these nanoflow rate experiments, ~ 0.1 $\mu\text{L}/\text{min}$ split flow was directed into a piece of pulled fused-silica capillary (150- μm o.d., 75- μm i.d., pulled to a 5- μm tip; New Objective, Cambridge, MA) where the ESI process took place directly from the pulled tip. In general, the ESI tip was positioned 2–3 mm away from the heated capillary orifice (185 $^{\circ}\text{C}$) and operated in positive ion mode at 1.8–2.4 kV. The ESI process was self-sustaining under these conditions and required no additional gas or sheath liquid.

Flow Injection Analysis. Single ion monitoring of m/z 407 was used to improve the precision and selectivity of the measurements. The electron multiplier voltage was set at 1000 V, and the scan rates were 0.3–0.4 s/scan. The HPLC pump used a flow rate of 200 $\mu\text{L}/\text{min}$ and was operated in isocratic mode where the ratio of A/B solvents was 20:80. Mobile phase A consisted of 10 mM ammonium acetate (adjusted to pH 4.7 with acetic acid), and mobile phase B was acetonitrile. In all cases, the injection volume was 10 μL .

For this experiment, four different solutions of 0.5 $\mu\text{g}/\text{mL}$ Carvedilol in 80% acetonitrile and 20% water were repeatedly flow injected. One solution contained nothing but Carvedilol (the

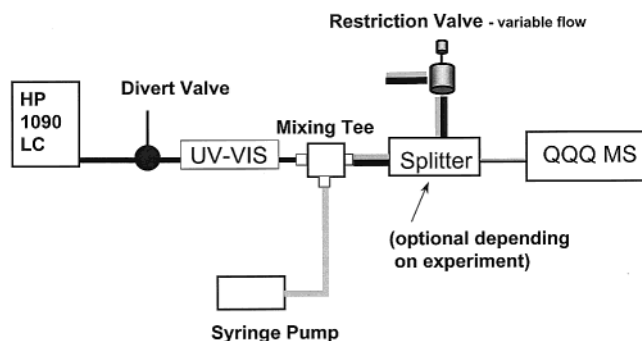


Figure 3. Block diagram of postcolumn addition experiment.

benchmark signal), while the other three solutions contained Carvedilol with possible suppressing agents. These individual solutions were flow injected and detected using an ESI-MS system where only the signal for Carvedilol was monitored. The agents that successfully suppressed the Carvedilol signal resulted in a peak area lower than that of the benchmark signal. Using peak area as a measure of signal, the ionization suppression from a variety of different substances could be directly compared. The solutions used, 80:20 acetonitrile/water, were as follows: (1) Carvedilol at 0.5 ng/ μ L; (2) Carvedilol at 0.5 ng/ μ L and taurocholic acid at 0.250 μ g/mL; (3) Carvedilol at 0.5 ng/ μ L and 1% DMSO (v/v); (4) Carvedilol at 0.5 ng/ μ L and Indinavir at 10 ng/ μ L.

The 200 μ L/min flow of carrier liquid was either directly introduced to the ESI-MS system or split to a lower flow rate and then introduced to the ESI-MS system. The split flow experiments used a custom-built concentric splitting device (discussed above) where the final split flows were 50, 5, and \sim 0.1 μ L/min. To both improve the accuracy of the data and generate statistical information, each of the four solutions was alternately injected 12 times at each of the flow rates in the following order: 1 2 3 4, 1 2 3 4, etc. This experimental design resulted in four data points/day for each of the four solutions. Repeating this experiments for 3 days resulted in a total of 12 data points ($n = 12$) for each of the solutions. Generating numerous data points enabled one to determine the validity and statistical repeatability of these measurements.

Postcolumn Addition. In this second set of experiments, bile was injected onto a LC column so that the suppression effects of its components on Carvedilol could be observed on-line with ESI-MS. As in experiment I, single ion monitoring (m/z 407) was used to improve the precision of the measurements. The electron multiplier voltage was set at 1000 V, and the scan rates were 0.3–0.4 s/scan. A general schematic of the experimental setup is presented in Figure 3. This figure contains details of the physical components of the system and is implicitly referenced throughout the following experimental description.

The HPLC pumped at a flow rate of 200 μ L/min and was operated in gradient elution mode. Mobile phase A consisted of 10 mM ammonium acetate (adjusted to pH 4.7 with acetic acid), and mobile phase B was acetonitrile. Mobile phase B was held at 10% for the first 2.2 min and then was increased linearly to 90% in 23 min. Subsequently, mobile phase B was held at 90% for 3 min giving a total run time of 28 min. Injections (10 μ L) of 50:50 bile/ CH_3OH (v/v) were made onto the LC column where the eluted bile components were detected using UV-DAD detection. A postcolumn switching valve was used to divert salts and other unretained analytes away from the MS (i.e., switched off-line) at

the beginning of the run. The system was brought back on-line 2.2 min after the sample was injected.

A syringe pump was used to deliver a constant stream of Carvedilol to the column effluent. The Carvedilol solution (5 μ g/mL) was infused at 7 μ L/min. This technique, referred to as postcolumn addition, has been previously reported for the addition of matrix components in flow FAB MS experiments.^{11,26} The column effluent and PCA solution were thoroughly mixed using a chromatographic mixing tee. Following mixing, the stream was either directed toward the ESI-MS system or split using the aforementioned splitting devices and then delivered to the ESI-MS system.

The PCA technique provided a constant delivery of analyte to the MS detector that resulted in a baseline signal in the MS TIC chromatogram. As the bile matrix components eluted from the column, they were mixed with the constant flow of Carvedilol (Figure 3) at the tee junction and then were introduced to the mass spectrometer. Using the signal of Carvedilol as a baseline, suppression effects from eluting bile components were readily observed as depressions in the Carvedilol signal. The expected outcome was an inverse peak that is a direct result of signal suppression effects from eluting matrix components. In this way, both the location and extent of suppression from bile components could be determined.

This experiment was conducted at 200, 50, 5, and 0.1 μ L/min in order evaluate suppression effects at various flow rates. The 200 μ L/min flow was directly introduced to the ESI-MS system whereas the other flows required a split. These LC-MS PCA experiments with Carvedilol were conducted in triplicate at each of the flow rates.

Indinavir Metabolites by LC-MS. Indinavir metabolites derived from microsomal incubations were analyzed by LC-MS using a Waters (Milford, MA) Symmetry C₁₈ reversed-phase LC column (2.1 mm \times 150 mm \times 3.5 μ m). Injection volume was 100 μ L; the pump flow rate was 200 μ L/min, and the pump operated in a gradient elution mode. Mobile phase A consisted of 10 mM ammonium acetate (adjusted to pH 4.7 with acetic acid), and mobile phase B was acetonitrile. The characterization of metabolites used a linear gradient: 15–40% B over 52 min, subsequently adjusted to 65% B in 13 min.

LC-MS experiments of Indinavir metabolites derived from in vitro sources were conducted at two different flow rates, 200 and 0.1 μ L/min, where the latter used a concentric splitting device to adjust the flow toward the MS. In this experiment, the solution containing metabolites (described above) was diluted with water 1:1 by volume. The solution was injected (100 μ L) onto the LC-MS system for analysis at 200 and 0.1 μ L/min in SIM mode. Ions of m/z 445, 482, 523, 539, 614, and 630 were monitored at a dwell time of 0.066 s, resulting in a total scan time of 0.4 s for the six masses. The MS was tuned with an Indinavir solution ($\sim 1 \times 10^{-6}$ M) pumped in at a flow rate of 40 μ L/min for the 200 μ L/min experiments and 0.1 μ L/min for the 0.1 μ L/min experiments. All LC-MS experiments were performed in triplicate, and the resulting chromatograms were not smoothed in order to allow visual comparison of signal-to-noise ratios. The information obtained from these analyses was used to calculate the differences in signal intensity and signal suppression between high and low flow rates.

(26) Coutant, J. E.; Chen, T. M.; Ackermann, B. L. *J. Chromatogr.* **1990**, 529, 265–75.

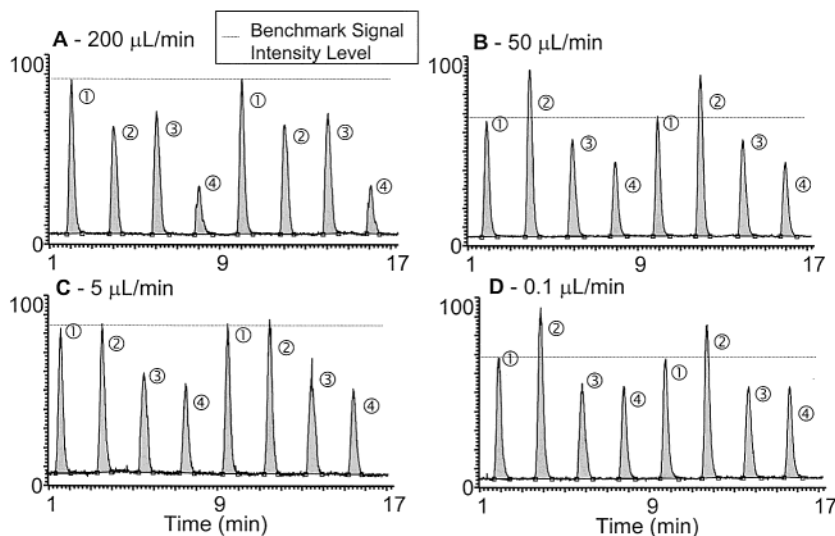


Figure 4. Flow injection profile for Carvedilol at (A) 200, (B) 50, (C) 5, and (D) 0.1 $\mu\text{L}/\text{min}$. Single ion monitoring mode of m/z 407.

RESULTS AND DISCUSSION

Flow Injection Analysis. In this experiment, Carvedilol, in solution by itself or in combination with another component, was repeatedly injected into the MS using an FIA format. Since all the test solutions contained the same concentration of Carvedilol, one would expect to see similar signal responses in each of these solutions. However, if ionization suppression processes were occurring in the presence of other agents, the Carvedilol response would be expected to decrease. The results of the flow injection experiments are presented in three basic formats (Figures 4–6). The different formats allow interpretation of the data in terms of splitter chromatographic properties, absolute signal intensity, and percent signal suppression. In the first format, the TIC for each solution was plotted at each flow rate (Figure 4). The effect of the concentric splitter on peak width and peak symmetry was evaluated rigorously and the results of such evaluation revealed no observable differences in peak shape. The TIC format shows that all peak widths are identical across the range of flow rates (i.e., peak widths or shapes are not dependent on the split ratio). We can conclude that the concentric splitting device did not degrade or alter chromatographic performance and, therefore, allowed for direct comparison of signal between the different flow rates. More importantly, these data show that the splitting device is capable of maintaining peak efficiency under extremely high split ratios (2000:1 for the 0.1 $\mu\text{L}/\text{min}$ split flow). The practical implications of this will be summarized later.

In the second format, the effect of flow rate on the absolute signal intensity is illustrated in the bar graph shown in Figure 5, where the average peak area for each solution is plotted for all four flow rates. As the ESI flow is decreased from 200 to 50 to 0.1 $\mu\text{L}/\text{min}$, the Carvedilol response increased in solutions 1–3. In all cases the 0.1 $\mu\text{L}/\text{min}$ flow rate yielded the highest Carvedilol signal intensity. In the best case, the TCA solution 2, compared at 200 and 0.1 $\mu\text{L}/\text{min}$, showed a 3-fold improvement in signal. In the case of solution 4 (Carvedilol plus Indinavir), there was no significant improvement in signal following reduction of flow from 200 to 0.1 $\mu\text{L}/\text{min}$. This suggested that a 20-fold excess of Indinavir does not have a negative effect on Carvedilol response. The measurements made here indicate that concentration sensitivity

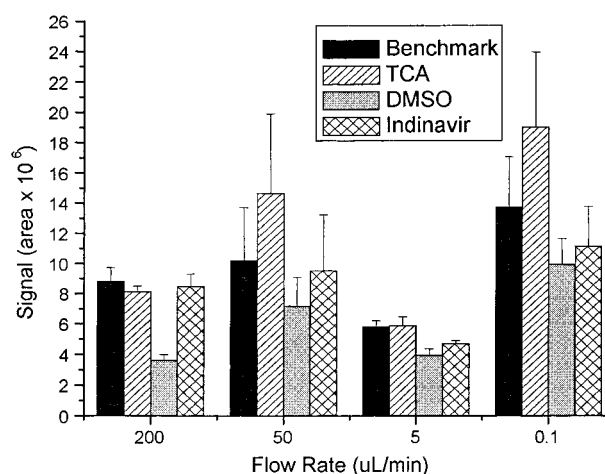


Figure 5. Peak area response vs flow rate for Carvedilol in the solutions that contain either Carvedilol alone (benchmark signal) or Carvedilol with a suppressing agent present TCA, DMSO, or Indinavir.

can be significantly improved by simply splitting the flow rate down to 0.1 $\mu\text{L}/\text{min}$. Moreover, the overall mass sensitivity can be improved by more than a factor of 2000 by splitting from 200 to 0.1 $\mu\text{L}/\text{min}$. In this fashion, precious sample can be collected for further analysis or used later as a reference standard. While the nanoliter per minute flow yielded the most abundant signal, the results did not demonstrate a linear relationship between decrease in flow rate versus increase in signal intensity. The reasons for this nonlinear relationship are unclear, and further experiments are required to determine why the 5 $\mu\text{L}/\text{min}$ flow did not fit the trend. We speculate that the dimensions of the standard Finnigan orifice needle (365 mm o.d. \times 150 mm i.d.) were not optimal for this flow, and therefore, improvements in signal intensity were not observed.

In the third format, shown in Figure 6, a plot of the percent signal suppression versus flow rate is presented for each solution. These measurements allow quantitative comparisons of the signal suppression observed at 200, 50, 5, and 0.1 $\mu\text{L}/\text{min}$ (the x -axis, not drawn to scale, shows the flow rate and the y -axis is percent signal suppression). To calculate percent signal suppression the

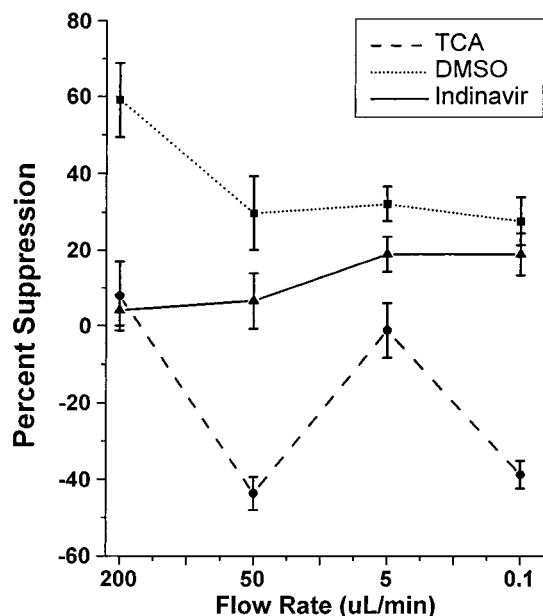


Figure 6. Flow rate vs percent signal suppression for Carvedilol in the solutions that contain Carvedilol with a suppressing agent present TCA, DMSO, or Indinavir.

following equation was used:

$$\% \text{ signal suppression} = 1 - \left(\frac{\text{suppressed signal area}}{\text{benchmark signal area}} \times 100 \right)$$

The graph reveals that several parameters may influence this degree of ion suppression as a function of flow rate. For example, ion suppression due to DMSO decreases significantly at reduced flow rates. On the other hand, the effect due to Indinavir is much less pronounced. Finally, TCA shows no clear trend other than a marked improvement when the percent signal suppression between the 200 and 0.1 mL/min flow rates was compared. It is clear from this limited set of data that more comparisons will have to be made in order to establish well-defined trends. However, it is significant to point out that these results were repeatable over a period of several days (also note RSD values given in Figure 6). Moreover, irrespective of the overall percent suppression trends, there is a clear and significant improvement in absolute signal when the results from flow rates of 200 versus 0.1 $\mu\text{L}/\text{min}$ are compared: specifically, note improvements in the Carvedilol signal, 175% (± 48) in the presence of DMSO, 30% (± 30) in the presence of Indinavir, and 133% (± 60) in the presence of TCA. As before, the 5 $\mu\text{L}/\text{min}$ flow did not fit the trend of improved resistance to suppression at low flows. This observation further corroborates the hypothesis that the ESI needle used did not have the optimum dimensions for 5 $\mu\text{L}/\text{min}$ flow.^{1,27}

Postcolumn Addition. The purpose of this experiment was to determine both the retention time and magnitude of suppression from individual components present in bile and to evaluate how those parameters changed as a function of flow rate. Suppression effects from eluting components were observed as a reduction in signal and, hereafter, these chromatograms will be referred to as "suppression chromatograms."

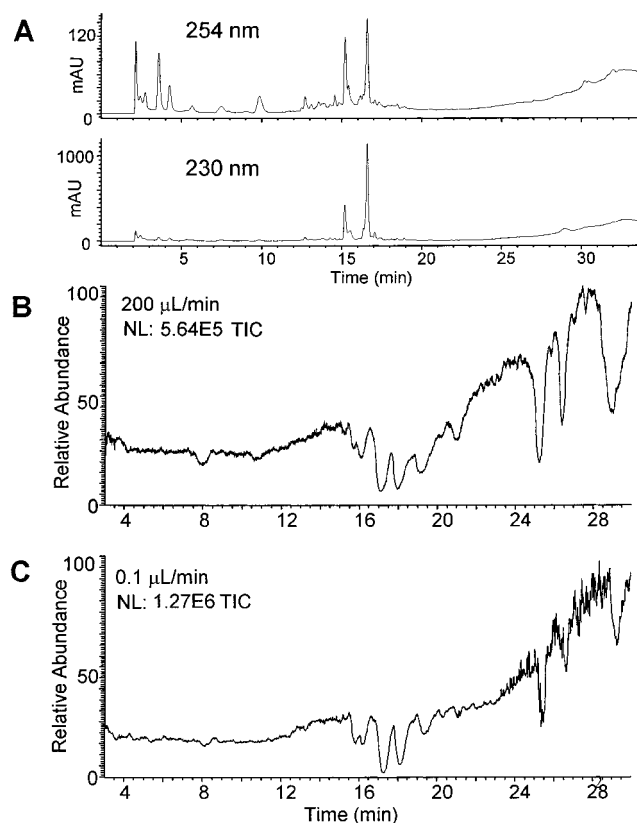


Figure 7. (A) LC-UV chromatogram at 254 and 230 nm of a 10- μL injection of 50% bile/50% methanol (v/v). (B) LC-MS chromatogram of a 10- μL injection of bile with postcolumn addition of Carvedilol. Single ion monitoring of m/z 407 at a flow rate of 200 $\mu\text{L}/\text{min}$. (C) LC-MS chromatogram of a 10- μL injection of bile with postcolumn addition of Carvedilol. Single ion monitoring of m/z 407 at a flow rate of 0.1 $\mu\text{L}/\text{min}$.

The LC-UV chromatogram of separated bile components at 230 and 254 nm (Figure 7A) indicates that several UV-absorbing species are present in bile. However, this method does not necessarily detect all compounds that are likely to cause ionization suppression. Several components present in bile, such as cholic acid and taurocholic acid, are invisible to UV and therefore could go unnoticed in a UV-DAD experiment. Hence, UV traces alone are not necessarily good indicators for the presence of possible suppressing agents. Furthermore, the data will show that UV absorbance (intensity) does not necessarily correlate with degree of ionization suppression.

The suppression chromatogram for the 200 $\mu\text{L}/\text{min}$ flow into the MS is shown in Figure 7B. Negative peaks observed at several points, including 17, 18, 25, and 29 min, in the chromatogram demonstrated the apparent suppression of the Carvedilol signal by eluting bile components. From these data, one can determine that there are several species present in bile that are capable of causing severe reduction in analyte response. In addition, the suppression chromatogram also indicates how the intensity of the Carvedilol signal varies as a function of LC run time or, more appropriately, mobile-phase composition. The plot displays an increase in signal intensity as the percent organic solvent increases. The signal intensity increased with the percent organic as a general trend across all flow rates, most likely the result of improved desolvation of ESI droplets at higher organic compositions.

(27) Van Berkel, G. J. *J. Am. Soc. Mass Spectrom.* **2000**, *11*, 951–60.

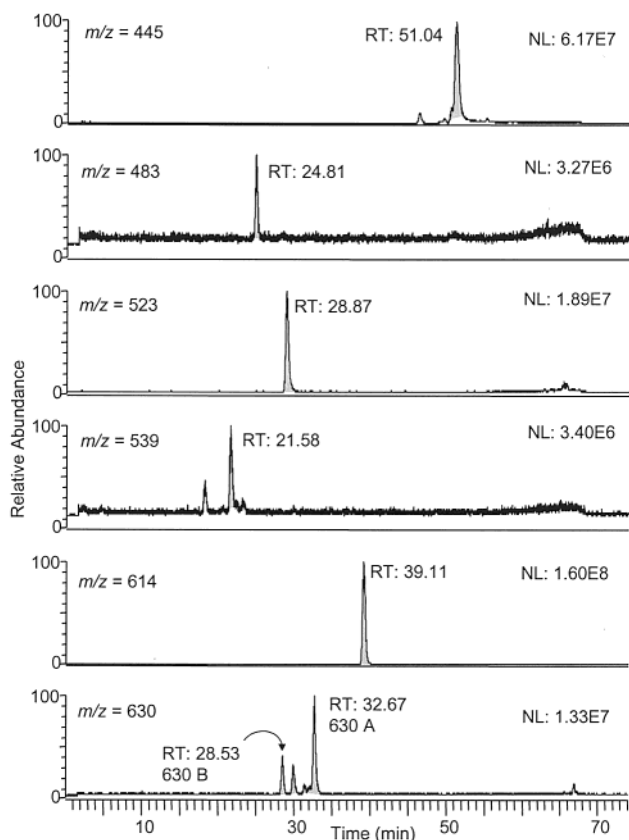


Figure 8. Extracted ion chromatograms for Indinavir metabolites generated from a rat liver microsomal incubation (m/z 445, 483, 523, 539, 614, and 630). The peaks detected here at 200 $\mu\text{L}/\text{min}$ are targeted for further analysis by SIM analysis at 200 and 0.1 $\mu\text{L}/\text{min}$ as shown in Figure 9.

Comparing the negative peaks observed at 200 $\mu\text{L}/\text{min}$ to those observed at 0.2 $\mu\text{L}/\text{min}$ (Figure 7C), it is evident that the overall signal intensity is ~ 2 -fold higher at lower flow rate and there was less signal suppression. Some depressions were clearly less intense, while others were simply narrower and exhibited a more rapid return to baseline. As in the previous experiments, the 5 $\mu\text{L}/\text{min}$ flow rate again did not exhibit a behavior consistent with the expected trends, suggesting that perhaps the source design was not optimal for ESI conditions at that flow rate.

Indinavir Metabolites by LC–MS. In this last experiment, metabolites generated from an *in vitro* incubation of Indinavir with rat liver microsomes were examined by LC–MS at 200 and 0.1 $\mu\text{L}/\text{min}$. The purpose of this experiment was to provide a real world application of flow splitting and present the associated benefits over conventional flow ESI–MS. The metabolites, previously characterized and reported by Koudriakova et al.,²⁴ were detected by SIM at m/z 445, 482, 523, 539, 614, and 630. After recording the metabolite peak intensities by area and height, comparisons of signal were made between the high and low flow rates. The incubation mixture was first analyzed by full-scan LC–MS (200 $\mu\text{L}/\text{min}$ ESI flow) in order to locate and confirm the presence and retention times of Indinavir metabolites. A series of reconstructed ion chromatograms representing the metabolites of Indinavir is shown in Figure 8. The drug-related peaks, which were to be evaluated at 200 and 0.1 $\mu\text{L}/\text{min}$ are highlighted. Consistent with the observations of Koudriakova et al.,²⁴ there

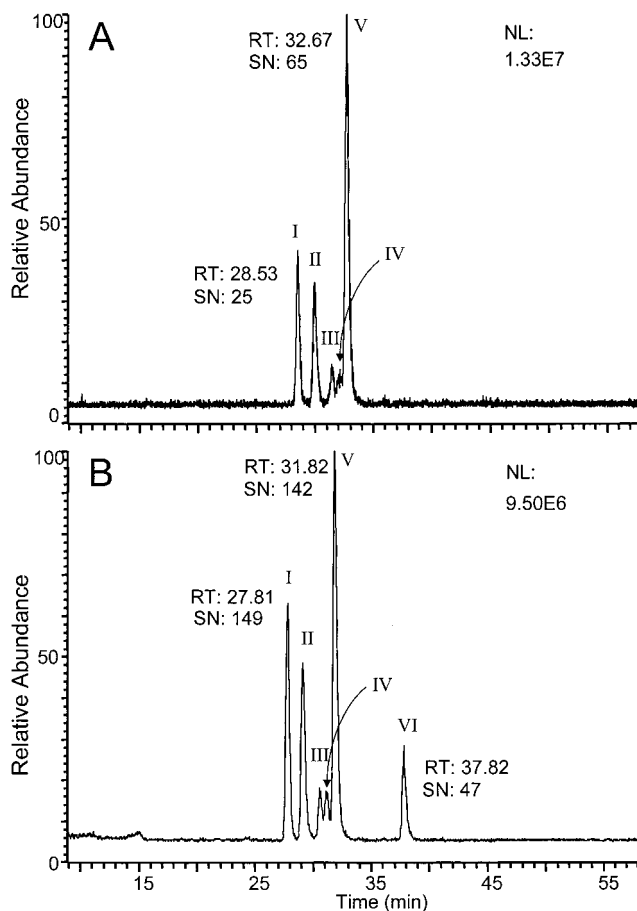


Figure 9. Extracted ion chromatograms for hydroxylated Indinavir metabolites (m/z 630) at (A) 200 and (B) 0.1 $\mu\text{L}/\text{min}$.

are numerous hydroxylated metabolites present in the metabolite mixture (m/z 630). Only the two marked 630A and 630B will be used in these comparisons.

Before examining the chromatograms for signal intensity, the mass traces for hydroxylated metabolites (m/z 630) were inspected to once again establish the integrity of the peak shape after a split of 2000:1. Figure 9 shows a side-by-side comparison of the extracted ion chromatograms for m/z 630 at 200 (A) and 0.1 $\mu\text{L}/\text{min}$ (B). The figure reveals that there is a cluster of at least five hydroxylated metabolites present in the mixture and that several peaks are not well resolved from one another. This situation provides an ideal circumstance for viewing changes in chromatographic performance because ill-defined peaks become less distinct when peak broadening is observed. Comparing Figure 9A and B, it becomes obvious that the splitting device not only maintained chromatographic quality but actually made these peaks more distinguishable from one another. In fact, the lower flow rate into the MS more clearly depicts the presence of the low-intensity peak (marked with an arrow) off the left shoulder of the intense peak at 31.82 min in Figure 9B. This effect is most likely due to the improved signal-to-noise ratio observed under nanoflow conditions resulting in a more well-defined peak. More rigorous inspection of these metabolite peaks, however, indicates that there is no measurable difference in peak width between the two flow rates (e.g., peak width at half-maximum). This example clearly documents the nanosplitter's ability to accurately maintain peak profiles at split ratios of $\sim 2000:1$.

The nanoliter per minute flow also revealed a putative hydroxylated metabolite (Figure 9B at 37.82 min) that was not previously observed at 200 $\mu\text{L}/\text{min}$. Since this peak had a retention time close to that of the parent drug, it is likely that the signal for this metabolite was previously suppressed by the parent drug. However, this peak could also be a noise/ghost peak resulting from the coeluting parent drug peak during low-flow analysis. For example, if an ammoniated adduct, $[\text{M} + \text{NH}_4]^+$, of the parent drug were present at high enough abundance, it could produce a signal misconstrued to be a hydroxylated metabolite. The ammoniated adduct of the parent drug would yield an m/z ion of 631 where the hydroxylated metabolites are detected at m/z 630. The close proximity of these two ions could lead to "ion crosstalk" if the resolution on the MS is not at or above 1 Da. To conclusively determine the nature of this peak, MS/MS experiments of the m/z 630 ion were performed at 0.1 $\mu\text{L}/\text{min}$. The MS/MS experiments revealed that this peak is in fact a hydroxylated metabolite that was previously undetected at 200 $\mu\text{L}/\text{min}$. The MS/MS spectrum of the metabolite (data not shown) has many common fragments as Indinavir (e.g., m/z 188, 364, and 465) as well as many fragments that are 16 Da higher than those observed from Indinavir (e.g., m/z 320 \rightarrow 336, 338 \rightarrow 354, 403 \rightarrow 419, 421 \rightarrow 437, 495 \rightarrow 511, and 513 \rightarrow 529).

In line with the experimental results discussed in the previous sections, it is reasonable to attribute the dramatic signal improvement shown in Figure 9B to an overcoming of ion suppression effects due to matrix. This hypothesis is also supported by consideration of the peak ratios in the mass chromatograms in Figure 9. Specifically, note that the ratios of the first five peaks (I–V) in Figure 9A are essentially identical to those in Figure 9B. Peak VI, which is completely absent in the chromatogram of Figure 9A, "shows up" with greater relative intensity than peaks III and IV, which coincidentally were present in Figure 9A. Based on these observations, such an improvement in sensitivity may be explained, at least in part, by a reduced competition from the large excess of parent drug whose elution time partially overlaps that of metabolite peak VI (see Figure 8 for a comparison of elution times).

To assess the nanosplitter's ability to generate improved signal over that of conventional flows, the peak areas and heights were determined for each of the metabolites detected in Figure 8. The data for these measurements are presented in Table 1 and contain peak intensity by height and area for each of the m/z values at 200 and 0.1 $\mu\text{L}/\text{min}$. Shown in this table are the average peak intensities, average RSDs, and average percent signal improvement when using the nanosplitter. It is indeed the case that the majority of the metabolites detected here exhibit significantly higher signal intensities at 0.1 $\mu\text{L}/\text{min}$ than at 200 $\mu\text{L}/\text{min}$. In only one instance did the peak intensity decrease, e.g., m/z 630A, and this decrease was less than 31%. In one instance, m/z 523, the improvement in signal was greater than 360%. The average change in signal intensity for these metabolites was an increase of 155 and 145% by area and height, respectively. However, the lower flow did yield less precision than that of the higher flows (i.e., average RSD is slightly higher at the nanoliter per minute level). The 0.1 $\mu\text{L}/\text{min}$ flow had an average RSD of 25% and the 200 $\mu\text{L}/\text{min}$ had an average RSD of 19% by area (height values

Table 1. Integration Results for Indinavir Metabolites, m/z 445, 482, 523, 539, 614, 630A, and 630B, by Height and Area at 200 and 0.1 $\mu\text{L}/\text{min}$ ($n = 3$)

m/z	Height				improvement (%)
	200 $\mu\text{L}/\text{min}$		0.1 $\mu\text{L}/\text{min}$		
	mean height	RSD (%)	mean height	RSD (%)	
445	6.06×10^7	15.1	9.69×10^7	38.1	59.8
482	2.18×10^6	17.9	9.46×10^6	22.6	333.6
523	2.30×10^7	17.4	1.04×10^8	28.9	354.5
539	2.80×10^6	2.5	8.38×10^6	13.3	199.4
614	2.14×10^8	22.8	3.05×10^8	27.4	42.1
630 A	1.57×10^7	17.1	1.23×10^7	25.8	-22.1
630 B	5.49×10^6	11.7	8.05×10^6	28.1	46.7

m/z	Area				improvement (%)
	200 $\mu\text{L}/\text{min}$		0.1 $\mu\text{L}/\text{min}$		
	mean area	RSD (%)	mean area	RSD (%)	
445	2.32×10^9	24.7	4.10×10^9	15.7	76.7
482	5.68×10^7	13.1	2.73×10^8	25.5	381.1
523	6.54×10^8	20.5	3.03×10^9	30.1	363.1
539	6.94×10^7	17.6	2.13×10^8	18.9	206.1
614	5.81×10^9	24.7	7.75×10^9	31.6	33.3
630 A	3.90×10^8	12.9	2.69×10^8	22.7	-31.0
630 B	1.23×10^8	19.2	1.89×10^8	28.9	53.8

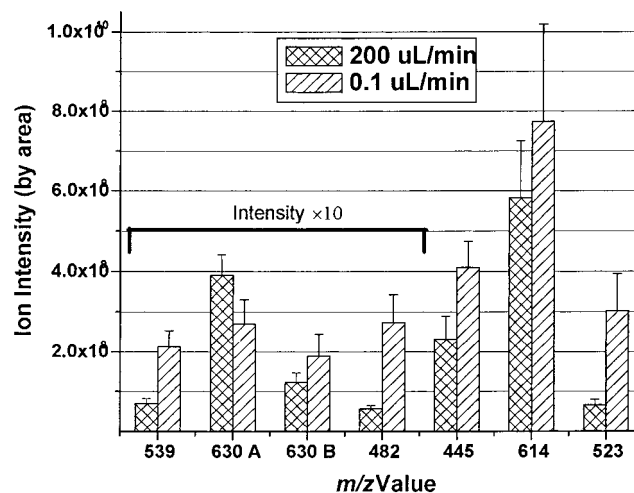


Figure 10. Bar graph for Indinavir metabolites, m/z 445, 482, 523, 539, 614, 630A, and 630B, by height and area at 200 and 0.1 $\mu\text{L}/\text{min}$.

yielded similar results). The data in Table 1 are also presented in bar graph format in Figure 10.

CONCLUSIONS

The sensitivity of detection and the efficiency of sample utilization determine the effectiveness of many trace level analytical applications that utilize HPLC. In HPLC–MS, exceptional mass sensitivity is achieved via the use of nano-ESI, which is compatible with nanobore chromatographic columns. On the other hand, there are many instances where the use of conventional-bore chromatographic methods is warranted. The latter requirements are typically associated with circumstances under which it is necessary to utilize larger injection volumes of a reconstituted physiological sample in order to introduce sufficient quantities of isolated trace level analyte into the LC–MS system. The nanosplitter device discussed in this paper provides a means for con-

ducting LC–MS analysis under nano-ESI conditions while utilizing conventional LC equipment and columns. It is shown that the nanosplitter can maintain chromatographic integrity at split ratios as high as 2000:1 and allows a comparison of signals over a wide range of flow rates. Most significantly, there was a significantly improved overall performance both in terms of absolute signal and in reduced signal suppression when the flow was decreased from 200 $\mu\text{L}/\text{min}$ to submicroliter per minute rates.

This work opens the door to a host of different applications and future related experiments. Future work will be directed toward further characterization of the system using other more complicated biological matrixes, further understanding of the underlying processes resulting in these flow related phenomena, improving performance and precision by optimizing the ESI tip dimensions, ESI high voltage, or both, and characterization of the

chromatographic integrity of the splitter waste stream. Other potential applications of this device may include on-line MALDI techniques where the use of conventional chromatography is desired but is not feasible because the source does not accept bulk LC flow rates²⁸ and techniques where the waste flow that contains sample is directed elsewhere for further measurement such as NMR or fraction collection equipment.

ACKNOWLEDGMENT

The authors thank Merck Research Laboratories for generously supplying Indinavir. This work was funded in part by a donation from GSK to the Barnett Institute and a grant (P.V.) from the National Cancer Institute (1R01CA69390). This is contribution number 795 from the Barnett Institute.

Received for review May 2, 2001. Accepted October 2, 2001.

AC010501I

(28) Preisler, J.; Foret, F.; Karger, B. L. *Anal. Chem.* **1998**, *70*, 5278–87.